Detection of density-dependent growth and fecundity of helminths in natural infections

A. W. SHOSTAK[1] *and* M. E. SCOTT[2]

[1] *Department of Zoology, University of Alberta, Edmonton, Alberta T6G 2E9, Canada*
[2] *Institute of Parasitology, Macdonald Campus of McGill University, 21111 Lakeshore Road, Ste-Anne de Bellevue, Québec H9X 1C0, Canada*

(*Received 25 March 1992; revised 27 November 1992; accepted 27 November 1992*)

SUMMARY

Density-dependent constraints on parasite growth, survival or reproduction are thought to be important in preventing the unchecked increase in parasite numbers within individual hosts or host populations. While it is important to know where, and with what severity, density dependence is acting within the parasite life-cycle, interpretation of data from natural infections is difficult. In this paper, we present a Monte Carlo simulation technique for examining such data for evidence of density dependence. We also describe how this technique may be used to distinguish among mechanisms hypothesized to generate density-dependent phenomena.

Key words: density dependence, fecundity, growth, models.

INTRODUCTION

Density dependence is recognized as an important factor in parasite population biology that prevents an exponential increase in parasite population size through effects on the establishment, reproduction or survival of individual parasites as a function of the number of other individuals within the same host (Keymer, 1982). In the case of reproduction, density dependence can occur through direct effects on the *per capita* egg production of individuals or indirectly through decreased growth, delayed maturation and/or reduced life-span of the parasite. Evidence for density dependence exists for a wide range of parasites (see reviews cited by Keymer, 1982; Scott & Lewis, 1987). It may result from competition among parasites for host resources (see for example Smith, 1984), from host immunological responses (Wakelin, 1986) and/or from direct parasite–parasite interactions (see for example Zavras & Roberts, 1985).

Rational design of control strategies for helminths of human and veterinary concern requires knowledge of the form and severity of density dependence (Keymer, 1982; Smith, 1984; Medley & Anderson, 1985; Dietz, 1988). However, in many situations it is impractical or unethical to do the experimental infections necessary to provide this information. In the context of human gastrointestinal nematodes, relevant data are usually obtained by quantifying parasite egg production in faecal samples, then counting expelled worms following anthelmintic treatment (Keymer & Slater, 1987). Interpretation of these data can be problematic because of variation among hosts in estimated *per capita* egg production of parasites, even when intensities of infection are similar. This may be due to inherent errors in egg counts (Hall, 1982; Sinniah, 1982) and in recovery of adult parasites (Keymer & Slater, 1987), or to heterogeneity of the host population (Keymer & Slater, 1987). An additional complication comes from sampling biases associated with the aggregated distribution of helminths in the host population (Keymer & Slater, 1987).

This study was stimulated by a provocative paper by Keymer & Slater (1987). They suggested that an illusion of density dependence could be generated by heterogeneity among hosts and high numbers of lightly infected hosts. In examining their paper, it was clear that a fundamental factor had been disregarded, namely the inherent differences in reproductive capacity among individual parasites (Dobson, 1985; Shostak & Dick, 1987; Jackson & Tinsley, 1988). While a low average parasite fecundity per host can indeed indicate a density-dependent depression of the fecundity of individual parasites within that host, it might also indicate simply the chance occurrence of many parasites with low inherent reproductive capacity. The relationship between the fecundity of individual parasites, and their average fecundity per host at various densities, is central to discriminating between these possibilities. We examined this relationship in a manner that permitted the use of an underlying theoretical framework for development of a practical test which uses data that can be obtained easily from naturally infected hosts. Average parasite fecundity is easily estimated from all hosts. More importantly, hosts

infected with one parasite also provide an indication of individual variation in fecundity among parasites that are under minimal influence of parasite density.

In this study, we develop a simulation technique for examining data from natural infections to determine the extent to which estimates of *per capita* egg production suggest density dependence. Then, we explore modifications of the technique that may permit discrimination among competing hypotheses regarding the mechanism(s) that generate density-dependent phenomena.

The approach we adopted is in part an extension of a study by Pacala & Dobson (1988). They used 95% confidence limits (C.L.), generated by simulation, to evaluate whether age-related changes in parasite intensity indicate density-dependent parasite-induced host mortality. We used a Monte Carlo simulation procedure to generate sets of data under different assumptions of density dependence. Using the simulated data, we calculated the average fecundity per host and examined the distributions of these values as intensity of infection increases. We also compared predicted patterns with sets of real data.

THE SIMULATION PROCEDURE

By simulation, we generated individual hosts with defined resources available to support the reproduction of their parasites. We gave each host a known number of parasites, and each parasite its own potential reproductive output. We assumed that the reproductive output of the parasite population is reduced below its potential, when the total reproductive potential of all parasites within a host exceeds the capacity of that host to support that reproductive effort. For convenience, this simulation is presented in the context of parasite productivity expressed as fecundity. The principle can be applied equally to other traits.

Definitions

N_j intensity, the number of parasites present in host, j.

$P_{\max,i}$ the maximum potential egg production of parasite, i (expressed/day or /g of faeces, or as egg content).

$P_{i,j}$ the number of eggs actually produced by parasite, i (expressed/day or /g of faeces, or as egg content) in host, j.

$P_{\text{avg},j}$ the mean *per capita* egg production of all parasites in host, j.

$P_{\text{net},j}$ total egg production of all parasites in host, j.

$H_{\max,j}$ maximum resources (expressed in same units as P) available in host, j, for use in parasite egg production.

It is important to note that the preceding terms are defined with respect to the host and parasite population **at the time they are sampled**. Samples of hosts harbouring a strongly seasonal parasite, for example, would have a lower $P_{\max,i}$ if the sample was taken when few worms had yet matured.

Assumptions

(1) The observed $P_{i,j}$ is determined by $P_{\max,i}$ of parasite, i, by $H_{\max,j}$ of host, j, and by N_j. (2) If $H_{\max,j}$ exceeds the combined $P_{\max,i}$ of all parasites in host, j, then each parasite will produce eggs at a level, $P_{\max,i}$, and the total egg production, $P_{\text{net},j}$ equals the combined $P_{\max,i}$. (3) If the combined $P_{\max,i}$ of all parasites in host, j, exceeds $H_{\max,j}$, resource limitations occur and reduce egg production by some or all parasites in host, j, such that $P_{i,j} \leqslant P_{\max,i}$ and $P_{\text{net},j} = H_{\max,j}$. (4) $P_{\max,i}$ and $H_{\max,j}$ may vary among parasites and among hosts, respectively. (5) Hosts acquire parasites independently of $P_{\max,i}$ and $H_{\max,j}$. (6) The appropriate sampling distributions for $P_{\max}$ and $H_{\max}$ are those that describe the range of characteristics of individual parasites and hosts **at the time the host population is sampled**.

The following decision rule was used to estimate $P_{\text{avg},j}$ in host, j:

$$P_{\text{avg},j} = P_{\text{net},j}/N_j, \tag{1}$$

where $P_{\text{net},j} = \Sigma P_{\max,i,j}$ when $\Sigma P_{\max,i,j} \leqslant H_{\max,j}$, and $P_{\text{net},j} = \Sigma P_{i,j} = H_{\max,j}$ when $\Sigma P_{\max,i,j} > H_{\max,j}$.

The Monte Carlo simulation to create hypothetical host–parasite assemblages involved the following steps. (1) Define sampling distribution for $H_{\max}$ as either normal or log-normal with given mean (μ) and standard deviation (σ). (2) Define sampling distribution for $P_{\max}$ as either normal or log-normal with given μ and σ. (3) Initiate creation of host, j, with N_j parasites. (4) Choose $H_{\max,j}$ at random from specified distribution of $H_{\max}$. (5) Choose $P_{\max,i}$ at random, N_j times, from specified distribution of $P_{\max}$, to become $P_{\max,1,j}$, $P_{\max,2,j}, \ldots, P_{\max,N,j}$. (6) Calculate $P_{\text{avg},j}$, using equation (1). (7) Repeat steps 3–6 for $j = 1000$ hosts. (8) Repeat steps 3–7 for $N_j = 1 \rightarrow 30$. (9) Using the 1000–$P_{\text{avg},j}$ values for each infection intensity, 95% C.L. were determined empirically as the highest and lowest values that were not included in the upper and lower 2·5% of observations.

It is important to note that the C.L. constructed from this simulation, for the special case of normally-distributed $P_{\max,i}$ with no density dependence, could equally be generated analytically. The standard deviation of the sample distribution of $P_{\text{avg},j}$ in this situation is the standard error (S.E.) of the mean for $P_{\max,i}$, given a sample size, j:

$$\sigma\,(P_{\text{avg},j}) = \text{S.E.}\,(P_{\max,i}) = \sigma\,(P_{\max,i})/\sqrt{j}, \tag{2a}$$

Table 1. Sampling distributions used in computer simulations

(Set numbers correspond to those used in text and figures.)

	P_{max}			H_{max}		
Set	Form*	μ	σ	Form*	μ	σ
1	N	1000	100	N	—†	0
2	N	1000	100	N	10000	1000
3	N	1000	100	N	2000	200
4	N	1000	500	N	—†	0
5	N	1000	500	N	10000	1000
6	N	1000	500	N	2000	200
7	L	6·9028‡	0·09975‡	N	—†	0
8	L	6·9028‡	0·09975‡	N	10000	1000
9	L	6·9028‡	0·09975‡	N	2000	200
10	L	6·796§	0·473§	N	—†	0
11	L	6·796§	0·473§	N	10000	1000
12	L	6·796§	0·473§	N	2000	200
13	N	1000	100	N	20000	2000
14	N	1000	100	N	20000	0
15	N	1000	0	N	20000	2000
16	N	1000	500	N	10000	3000
17	N	1000	500	L	9·1673¶	0·2936¶
18	L	6·796§	0·473§	N	10000	3000
19	L	6·796§	0·473§	L	9·1673¶	0·2936¶
20	N	1000	Variable‖	N	—†	0
21	N	1000	Variable‖	N	10000	1000
22	N	1000	Variable‖	N	2000	200

* N, normal distribution; L, log-normal distribution.
† Arbitrarily high value to eliminate density-dependent effect.
‡ Arithmetic equivalent: $\mu = 1000$; $\sigma = 100$.
§ Arithmetic equivalent: $\mu = 1000$; $\sigma = 500$.
¶ Arithmetic equivalent: $\mu = 10000$; $\sigma = 3000$.
‖ Variance increasing with intensity, j: $\sigma = (0{\cdot}1 + 0{\cdot}1\ (j-1))\ \mu$.

and the 95% C.L. are:

$$\mu\,(P_{\max,i}) \pm 1{\cdot}96 \times \text{S.E.}\,(P_{\max,i}). \qquad (2b)$$

These limits are relatively insensitive to departures of $P_{\max,i}$ from normality, due to the Central Limit Theorem (Sokal & Rohlf, 1981). Using the simulation to generate C.L. was more tedious than using the analytical approach. However, this method enabled us to use the same technique for comparison of predictions in the absence of density dependence, to predictions when density dependence was simulated.

RESULTS OF THE SIMULATIONS

Sampling distributions for the simulations represented various combinations of μ, σ, and form of distribution of P_{max} and H_{max}. A normal distribution was the basic form used, but many traits (including egg production) exhibit a positively skewed distribution (Dobson, 1985; Keymer & Slater, 1987; Shostak & Dick, 1987). Skew was simulated by drawing values from a log-normal distribution (discarding values more than 3 S.D. above the mean). The μ and σ chosen for skewed distributions had arithmetic μ and σ comparable to the normal distributions with which they were compared.

The sampling distributions of P_{max} and H_{max} for each simulation are summarized in Table 1, along with a code for reference among text, tables and figures.

Density independence

Density-independent data were simulated using a sampling distribution with $H_{\max,j} \gg \Sigma P_{\max,i,j}$ at all intensities. Variability in P_{avg} among simulated hosts, and the corresponding C.L., was widest in single-worm infections and declined rapidly as intensity of infection increased (Fig. 1, Sets 1, 4, 7, 10). The C.L. were symmetrical when P_{max} was normally distributed (Fig. 1A, B) or skewed with low variability (Fig. 1C), but were asymmetrical at low intensities when P_{max} were drawn from a skewed distribution with high variability (Fig. 1D). These results, supported by the Central Limit Theorem, suggest that changes in assumptions regarding the form of the sampling distribution of P_{max} in the parasite population will have relatively minor effects. Moreover, the asymmetry resulting from skewed P_{max} affected primarily the upper C.L., and it is the lower

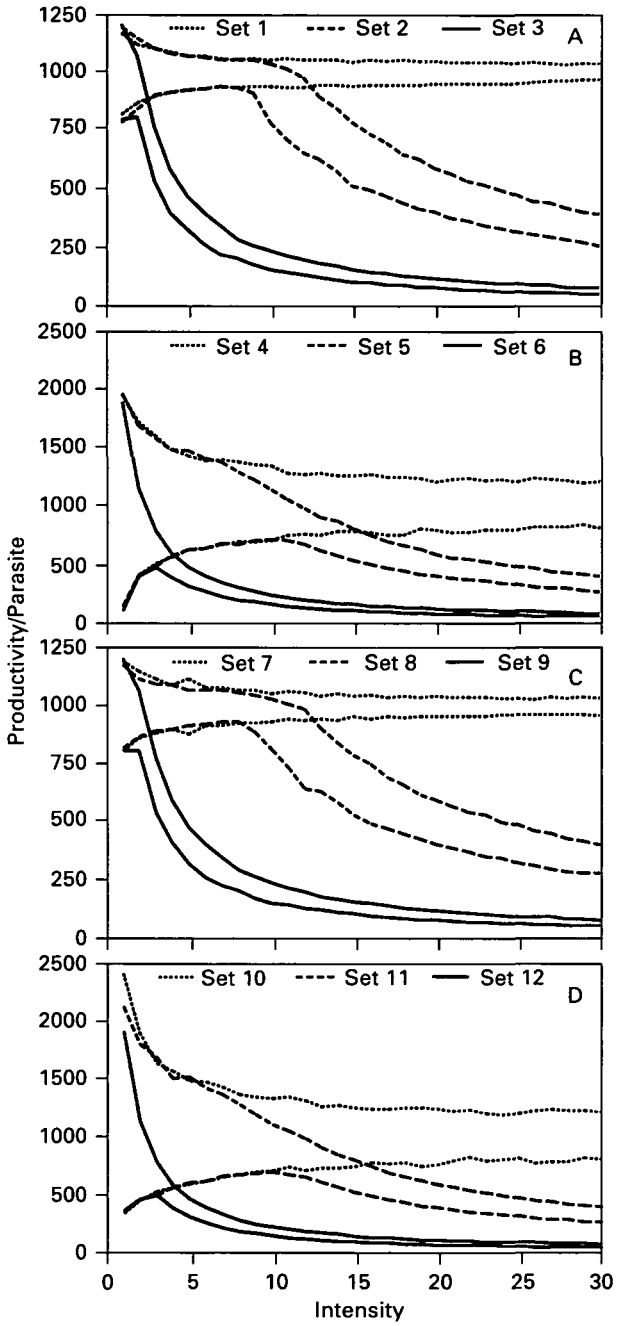

Fig. 1. Effect of sampling distribution of P_{max} on predicted 95% confidence limits for *per capita* parasite productivity. Set numbers refer to parameters described in Table 1. (A) Normal P_{max} with low variability. (B) Normal P_{max} with high variability. (C) Skewed P_{max} with low variability. (D) Skewed P_{max} with high variability. Each figure includes a simulation of no density dependence (.....), and density dependence at an intensity of 10 (----) or 2 (——).

C.L. that is of concern in detecting density-dependent effects. We interpret observations falling below the lower C.L. as representing an unusually small P_{avg} if the hypothesis of density independence is true.

Introduction of density dependence

To simulate density dependence, μ (H_{max}) was set to

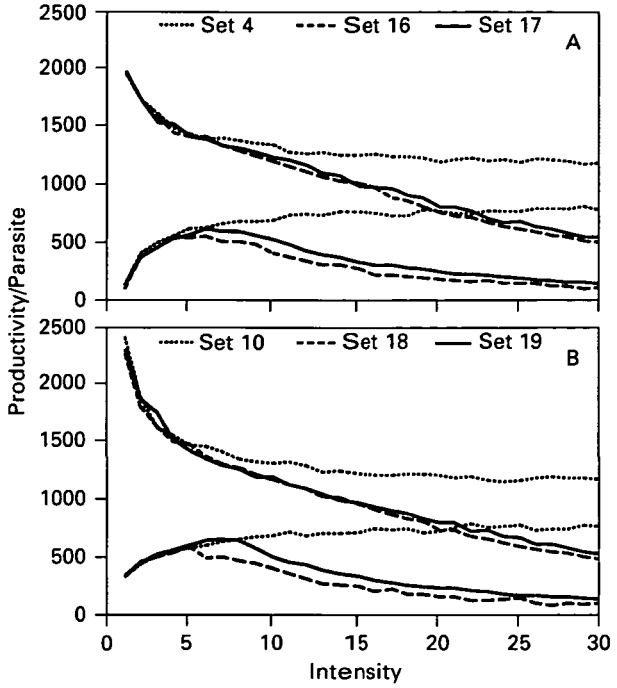

Fig. 2. Effect of sampling distribution of H_{max} on predicted 95% confidence limits for *per capita* parasite productivity. Set numbers refer to parameters described in Table 1. (A) Normal P_{max} with high variability. (B) Skewed P_{max} with high variability. Each figure includes a simulation of no density dependence (.....), and density dependence at an intensity of 10, with normal H_{max} (----) or skewed H_{max} (——).

levels that allowed $\Sigma P_{max,i,j}$ to exceed H_{max} in heavily infected hosts. P_{max} were sampled from normal distributions with low (Fig. 1A) and high (Fig. 1B) variability, and from skewed distributions with low (Fig. 1C) and high (Fig. 1D) variability. In all simulations, P_{avg} varied similarly with respect to parasite intensity and the severity of the density-dependent constraint (extent to which average H_{max} exceeded average P_{max}). *Per capita* egg production mirrored density-independent results at low intensities, and declined in a reverse-sigmoid fashion as intensity increased. When density dependence was severe (low H_{max}), P_{avg} dropped steeply (Sets 3, 6, 9, 12). When it was less severe (high H_{max}), the drop in P_{avg} occurred at higher intensities and was less steep (Sets 2, 5, 8, 11).

Additional simulations explored effects of the form of the distribution of H_{max}. Hosts with H_{max} drawn from normal (Fig. 2A) and skewed (Fig. 2B) distributions were paired with parasites drawn from normal (Sets 16, 18) and skewed (Sets 17, 19) distributions of P_{max}. The C.L. were similar in all cases, suggesting that changes in assumptions regarding the form of the sampling distribution for H_{max} would, as for P_{max}, have only minor effects.

A comparison of C.L. produced under assumptions of density independence and density dependence (Figs 1 and 2) shows overlap of C.L. at low intensities,

Table 2. Index of detectability of density dependence, *DI*, for each simulation

(Values for H_{max} and P_{max} are the mean and standard deviation, with the form of the sampling distribution indicated by N = normal and L = log-normal.)

	DI	
$H_{max} = 2000 \pm 200$ (N)		
$P_{max} = 1000 \pm 100$	1·4 (Set 3, N)	1·4 (Set 9, L)
$P_{max} = 1000 \pm 500$	2·2 (Set 6, N)	2·2 (Set 12, L)
$H_{max} = 10000 \pm 1000$ (N)		
$P_{max} = 1000 \pm 100$	1·2 (Set 2, N)	1·3 (Set 8, L)
$P_{max} = 1000 \pm 500$	1·6 (Set 5, N)	1·6 (Set 11, L)
$H_{max} = 10000 \pm 3000$ (N)		
$P_{max} = 1000 \pm 500$	2·1 (Set 16, N)	2·2 (Set 17, L)
$H_{max} = 10000 \pm 3000$ (L)		
$P_{max} = 1000 \pm 500$	2·1 (Set 18, N)	2·1 (Set 19, L)

but non-overlap at higher intensities. This suggests that, although the effects of density dependence may be indistinguishable from background variation at low intensities, the effects may be distinguishable statistically at higher intensities.

Detection of density dependence

Density-dependent effects likely manifest themselves gradually as intensity increases. Our concern is to determine the point where we can say with confidence that density dependence is occurring. Detectability may be impaired when the magnitude of effect and number of host individuals involved is low. We defined a 'detectability index', *DI*, to evaluate objectively the ability to detect density dependence in various situations: $DI = V2/V1$, where $V1 = \mu(H_{max})/\mu(P_{max})$, and $V2$ = minimum intensity for which the C.L. under assumptions of density independence and density dependence do not overlap. $V1$ is the maximum intensity at which the average H_{max} provides sufficient resources to sustain the average P_{max}, so we would predict density-dependent effects in an average host at an intensity $> V1$. $V2$ is the minimum intensity at which one would detect density dependence reliably, because *per capita* parasite fecundity in 95% of hosts is lower than that in 95% of hosts where density dependence is absent. *DI* is the multiple by which an observed intensity would have to exceed the intensity that first produces density-dependent effects, in order for *per capita* fecundity to decline significantly. Density dependence becomes more difficult to detect as *DI* increases from its minimum value of 1. A sample would need to include increasingly heavily infected hosts, yet these are the hosts that are infrequent in abundance.

Values of *DI* from the previous simulations (Table 2) varied according to the μ and σ of P_{max} and H_{max}, but were insensitive to assumptions regarding the underlying form of the distribution of P_{max} or H_{max}. Interactions were also evident. For example, an increase in σ (P_{max}) had a greater effect on *DI* when μ and σ of H_{max} were low.

The interaction of H_{max} and P_{max} on the ability to detect density dependence was explored in greater detail. We chose $\mu(P_{max}) = 1000$ and $\mu(H_{max}) = 2000$, 10000 or 20000, to simulate density dependence in an average host at 2, 10, or 20 parasites. Combinations of $\sigma(P_{max})$ and $\sigma(H_{max})$ were simulated at each $\mu(H_{max})$, and *DI* were calculated. Contour maps (Fig. 3) show that *DI* increased with any increase in the variation of H_{max} or P_{max}, but at different rates. As $\mu(H_{max})$ increased, *DI* became less sensitive to changes in variation of P_{max}, but more sensitive to variation of H_{max}. Maximum *DI* in these simulations were about 2·3, 2·1 and 1·8 (Fig. 3). It appears that, even under high levels of variation in P_{max} and H_{max}, density dependence would be detected if a sample included even one host with an intensity about 2× the intensity that causes density dependence.

Interaction of P_{max} and H_{max}

The simulated C.L. under density independence are a function primarily of parasite intensity and the variability of P_{max} among parasites. However, when density dependence occurs, variability of H_{max} among hosts affects the C.L. at higher intensities. It was just shown that the relationship between these two sets of C.L. determines the ability to detect density dependence. It was possible through simulation to separate the contributions of host and parasite variability (Fig. 4A). We compared a simulation where hosts and parasites were both variable (Set 13), to one where P_{max} only was variable (Set 14) and one where H_{max} only was variable (Set 15). The C.L. were determined by variation in P_{max} at low intensities, and by variation in H_{max} at high intensities. A clear combined contribution of H_{max}

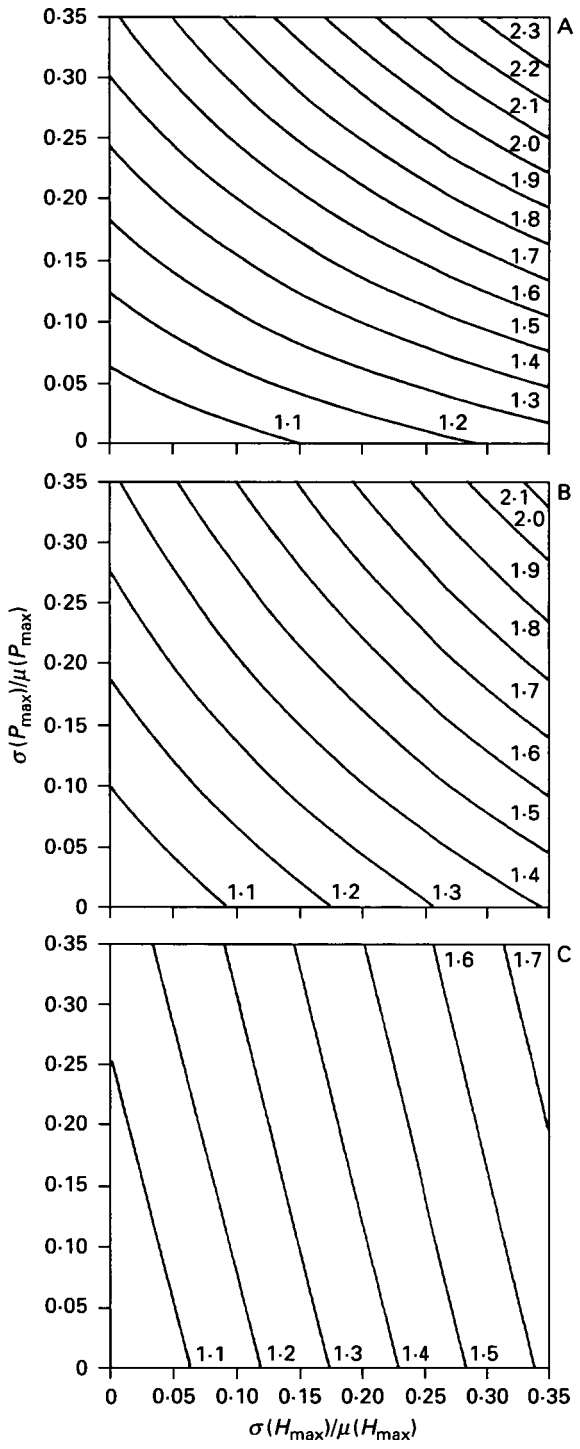

Fig. 3. Contour plots of *DI*, the detectability index for density dependence, as a function of the variability of P_{max} and H_{max}. (A) $\mu(P_{max}) = 1000$; $\mu(H_{max}) = 2000$. (B) $\mu(P_{max}) = 1000$; $\mu(H_{max}) = 10000$. (C) $\mu(P_{max}) = 1000$; $\mu(H_{max}) = 20000$. The variances, $\sigma(P_{max})$ and $\sigma(H_{max})$, are scaled relative to their respective means.

and P_{max} occurred only within a narrow intensity range where density dependence first occurred.

Extension of basic model

The basic model assumes constant μ and σ of P_{max} and H_{max} at all intensities. Modifications are incorporated easily. For example, one might evaluate the consequences of $\sigma(P_{max})$ that increases with intensity, but has constant $\mu(P_{max})$, i.e. density independence. The result (Fig. 4B, Set 20) is a widening of the C.L. at higher intensity. The degree of widening depends on the function used to relate variance to intensity. This wider C.L. reduces the ability to detect density dependence (compare Fig. 4B with Fig. 1A).

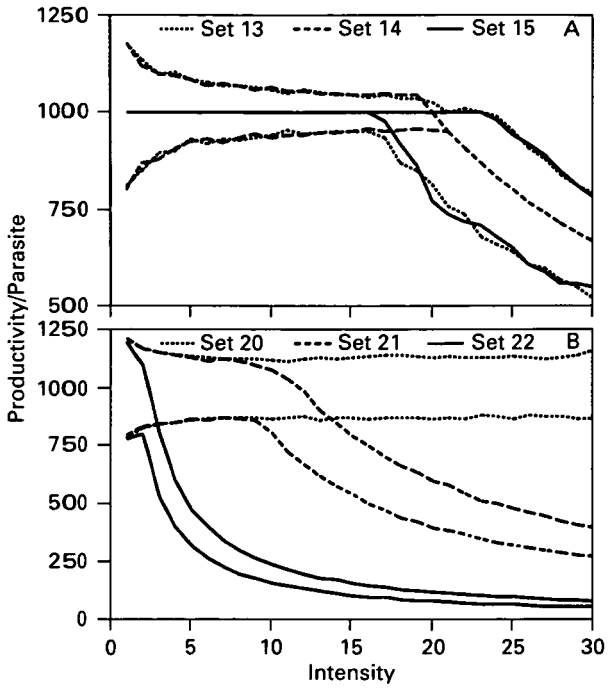

Fig. 4. Simulations to identify factors responsible for the width of confidence limits. Set numbers refer to parameters described in Table 1. (A) Variability in P_{max} only (----), H_{max} only (——) or P_{max} and H_{max} jointly (. . . . .). (B) Variance of P_{max} increasing with intensity, with no density dependence (. . . . .), or density dependence at an intensity of 10 (----) or 2 (——).

The basic model can be tailored to diverse biological situations by specifying user-defined functions for μ and σ of P_{max} and/or H_{max}. These could produce specific null hypotheses (density independence), or alternate hypotheses that specify density dependence through various mechanisms.

Summary of theoretical simulations

Assumptions concerning the form (normal versus log-normal) of the underlying distribution of P_{max} in the parasite population, or H_{max} in the host population, had little effect on the ability to detect density dependence. However, increased variability among parasites or hosts widened the C.L. for P_{avg}. Apparently, detection of density dependence is more difficult when the underlying variability among parasites in their intrinsic reproductive potential, or among hosts in their ability to support parasites, is high.

Table 3. Sampling distributions used to test hypotheses of density dependence on real data

(See text for details.)

Parasite	Hypothesis*	P_{max} Form	P_{max} Mean	P_{max} S.D.	H_{max} Mean	H_{max} S.D.
Triaenophorus crassus (egg content)	H_0	L	11·76	2·33	—	—
Proteocephalus pinguis (μg dry weight)	H_0	L	6·1	2	—	—
Protopolystoma xenopodis (daily egg output)	H_0	L	2·1	0·4123	—	—
Ascaris lumbricoides (eggs/g faeces)	H_0	L	5·1801	1·5847	—	—
Triaenophorus crassus (μm^3/1000 in female hosts)	H_0	N	2023	556	—	—
	H_a	N	2023	556	2450	686
Triaenophorus crassus (μm^3/1000 in male hosts)	H_0	N	2023	556	—	—
	H_a	N	2023	556	1750	473
Hymenolepis diminuta (weight units)	H_0	N	478	72	—	—
	H_{a1}	N	478	72	4792	479
	H_{a2}	N	Variable†	72	—	—
	H_{a3}	N	Variable†	72	4792	479

* H_0: null, no density dependence; H_a, H_{a1}: alternate, density dependence through resource limitation; H_{a2}: alternate, density dependence through intra-specific crowding factor: H_{a3}: alternate, density dependence through combination of resource limitation and intraspecific crowding factor.

† Mean decreasing with intensity, j: $\mu = 478\ (1-d)$; $d = 0{\cdot}75/(1+\exp(5-0{\cdot}4\,j))$.

RESULTS BASED ON REAL DATA SETS

To bring this theoretical approach closer to the 'real world,' we repeated the simulation procedure using P_{max} and H_{max} estimated from field and experimental data. A normal distribution was used if data were symmetrical in distribution, and a log-normal distribution if data were skewed. The sampling distributions are in Table 3. We then compared the observed data with C.L. generated under assumptions of density dependence or independence. We addressed two questions: (1) Can expected C.L. (under an assumption of density independence) provide insight into the expression of density dependence in field data? (2) Can a simulation approach provide insight into the mechanism(s) underlying the density dependence? We chose seven data sets from natural and experimental infections.

Triaenophorus crassus *fecundity*

The egg content of individual *T. crassus* (Cestoda), collected from naturally infected pike *Esox lucius*, was recorded by Shostak & Dick (1987). We estimated P_{max} from their raw data, by calculating egg content of individual worms present in fish with only 1 or 2 gravid worms. Simulated *per capita* productivity was expressed as the mean number of eggs per gravid worm. We simulated intensities of infection up to 25 worms/host (the maximum in the data set) and determined C.L. under a null hypothesis, H_0, of no density dependence. All observations but one fell within these C.L. (Fig. 5A). We suggest that these data show no indication of density-dependent reproduction.

Proteocephalus pinguis *weight*

Raw data on weights of individual *P. pinguis* (Cestoda), from natural infections of pike, were available from a study by Shostak (1986). Dry weight/worm was used as the measure of productivity. Few fish had single infections, so estimates for P_{max} were based on individuals in fish with fewer than 15 parasites. Again, an H_0 of no density dependence was used. The observed average worm weights/host (Fig. 5B) were outside the C.L. in 24 of the 98 hosts, in disagreement with this simple null hypothesis. However, the pattern of outliers was also inconsistent with density dependence. Most (19/24) of the outliers were above the C.L., and at low (< 100 worms) intensities; at higher intensities (> 100 worms), 1 observation was above, 5 within and 2 below the C.L.

Protopolystoma xenopodis *fecundity*

Jackson & Tinsley (1988) studied egg production by individual *P. xenopodis* (Monogenea) in experimental

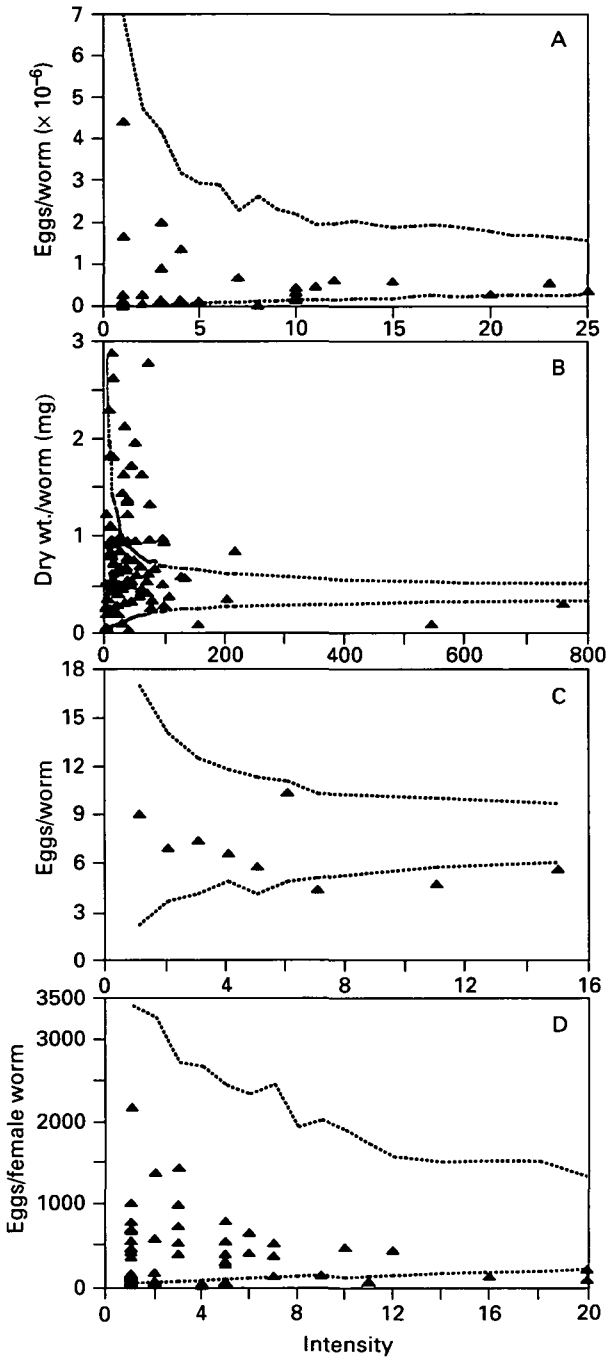

Fig. 5. Simulated 95% confidence limits under a null hypothesis (H_0) (.....) of no density dependence, applied to observations (▲) on four species of parasite. Parameters for the simulations are in Table 3. (A) Egg content of *Triaenophorus crassus* in the fish host. (B) Dry weights of *Proteocephalus pinguis* in the fish host. (C) Egg production by *Protopolystoma xenopodis* in the amphibian host. (D) Faecal egg output by *Ascaris lumbricoides* in man.

infections of *Xenopus laevis*. Mean egg output/day in single worm infections (taken from Fig. 3C of Jackson & Tinsley, 1988) was the estimate for P_{max}. The observed data were grand means across all hosts, at each intensity (taken from Fig. 6 of Jackson & Tinsley, 1988). These were compared with C.L. generated from the simulation under an H_0 of no density dependence (Fig. 5C). All means at intensities of 1–6 were within the C.L., but 2 of 3 means at intensities of 7–15 were just beneath the lower C.L. These data suggest weak density dependence, but more data from hosts infected with 7 or more parasites are needed. Jackson & Tinsley (1988) interpreted their data as suggesting two hypotheses: reduced resource availability that depressed *per capita* fecundity when as few as 2 worms were present, or a statistical phenomenon resulting from the distribution of samples. Our analysis supports the former hypothesis at higher intensities, the latter at lower intensities.

Ascaris lumbricoides *fecundity*

Per capita egg production by female *A. lumbricoides* (Nematoda) was determined by Holland *et al.* (1987). Faecal egg counts were followed by anthelmintic treatment to enumerate the female worms. Data from 51 of the 58 hosts plotted in Fig. 2 of Holland *et al.* (1987) could be resolved. We used data from 19 hosts harbouring a single female *A. lumbricoides* to estimate P_{max}. The C.L. resulting from a simulation under an H_0 of no density dependence (Fig. 5D) include 44 of 51 observations. The upper C.L. were well above the highest observations, suggesting that the skew of P_{max} was over-estimated. The deviant observations, which occurred at higher intensities, were slightly below the lower C.L. This suggests that weak density dependence was evident in the range of intensities sampled, and corroborates the interpretation of Holland *et al.* (1987). They used multivariate modelling and concluded that density-dependent constraints were evident, but not pronounced.

Triaenophorus crassus *procercoid volume*

Shostak, Rosen & Dick (1985) evaluated the volume of procercoids of *T. crassus* in experimental infections of female and male *Cyclops bicuspidatus thomasi*. Raw data from that study were used to evaluate parasite productivity. P_{max} was estimated as the volume of procercoids > 2 weeks old in single-worm infections of female hosts (even single-worm infections in male hosts appeared stunted). Observed mean procercoid volume/female host deviated markedly from C.L. generated under an H_0 of no density dependence (Fig. 6A). Half of the observations were below the lower limit at an intensity of 2, and all were below at intensities of 3–15. In male hosts, under the same H_0, two observations were below the C.L. in single-procercoid infections, and all observations were below the C.L. at intensities of 2–19 procercoids (Fig. 6B). Together, data from male and female copepods provide strong evidence for density-dependent effects on procercoid size. Given evidence

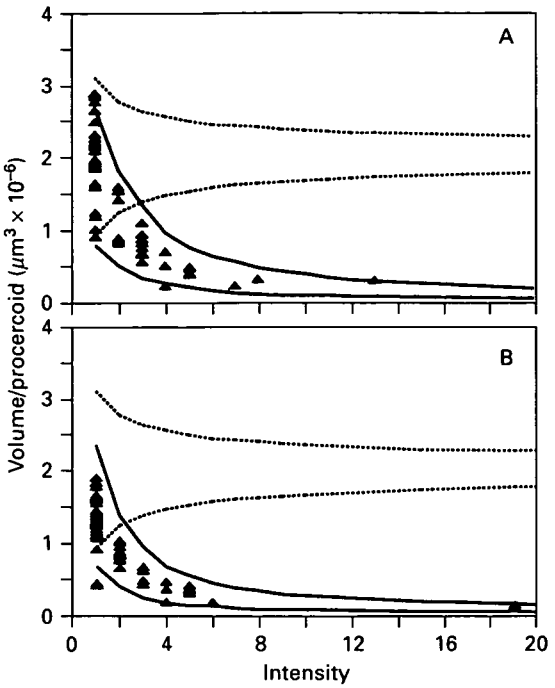

Fig. 6. Simulated 95% confidence limits under a null hypothesis (H_0) (.....) of no density dependence and an alternate hypothesis (H_a) (——) of density dependence based on resource limitation, applied to observations (▲) on mean volume of procercoids of *Triaenophorus crassus* in the copepod host. Parameters for the simulations are in Table 3. (A) Volume in female hosts. (B) Volume in male hosts.

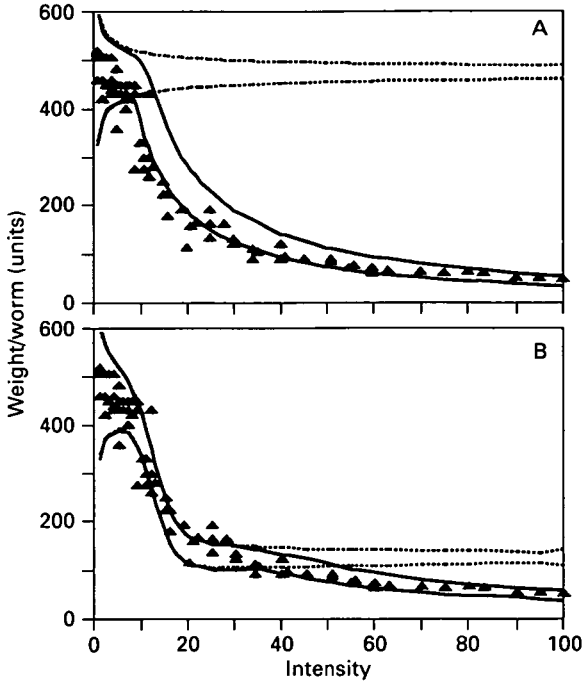

Fig. 7. Simulated 95% confidence limits for observations (▲) on mean weight of *Hymenolepis diminuta* in the rodent host. Parameters for the simulations are in Table 3. (A) A null hypothesis (H_0) (.....) of no density dependence, and an alternate hypothesis (H_{a1}) (——) of density dependence due to resource limitation. (B) Alternate hypotheses of density dependence, due to an intra-specific crowding factor (H_{a2}) (.....) or combined effects of resource limitation and an intra-specific crowding factor (H_{a3}) (——).

of density dependence, we repeated the simulation but assumed that density dependence, limited by H_{max}, was present. To do this, we estimated H_{max} in the same units (volume) as P_{max}, by using asymptotic total procercoid volume/host in female and male copepods (Shostak *et al.* 1985) to generate the alternate hypotheses, H_a. The C.L. under H_a included 46 of 50 observations from female copepods (Fig. 6A), and 49 of 52 observations from male copepods (Fig. 6B). These comparisons are consistent with the hypothesis that a single density-dependent factor, limitation in host size, affects body size of procercoids.

Hymenolepis diminuta *weight*

Read (1951) published a scatter plot of 'relative surface area' (defined as weight$^{\frac{2}{3}}$/weight) of the cestode *H. diminuta* versus intensity of infection in rats. We converted these values to weight (arbitrary units). Mean P_{max} was the mean weight of *H. diminuta* in the three hosts with single worm infections. From the literature, the coefficient of variation of mean weight in single-worm infections of *H. diminuta* averages about 15% (8·7–26·3% in Roberts (1961) 17·2% in Hesselberg & Andreassen (1975)); this was used to estimate S.D. (P_{max}). Read's data fell within the C.L. under an H_0 of no density dependence for hosts infected with fewer than 10 parasites (Fig. 7A), but all observations at higher intensities were below the lower C.L. This suggested strong density dependence in this system. We repeated the simulation, but with an alternate hypothesis, H_{a1}, of density dependence limited by H_{max}. H_{max} was estimated from total parasite weight in the most heavily infected hosts (intensity $\geqslant 50$). The C.L. under H_{a1} enclosed most values from rats infected with less than 10 or more than 25 parasites. However, data from intermediate intensities were below the lower C.L. We interpret this as suggesting density dependence, but not operating in accordance with the single resource limitation assumed in the model.

Studies *in vitro* and *in vivo* on thymidine uptake in the neck region of *H. diminuta* (Roberts & Insler, 1982; Zavras & Roberts, 1985; Cook & Roberts, 1991) suggest the presence of an intraspecific 'crowding factor'. We used this phenomenon to illustrate one way in which our basic simulation model can be modified to evaluate alternative causal mechanisms of density dependence. Data from Roberts & Insler (1982) suggest that production of the putative crowding factor is density dependent.

Based on their data, we predicted qualitatively that inhibition of P_{max} due to the crowding factor should initially increase rapidly with intensity, then increase at a lower rate, but be unable to completely suppress growth. For illustrative purposes we used a logistic function to describe growth depression relative to intensity, with parameters that produced a maximum depression of 75%, approximating the reduction in thymidine uptake (Roberts & Insler, 1982) observed using crowding factor from 100-worm infections. This second alternate hypothesis, H_{a2}, was identical to H_0 except the mean P_{max} was affected by the crowding factor. The C.L. under H_{a2} (Fig. 7B) excluded only 8 observations at intensities < 30 worms, a reasonable fit, but excluded all observations at intensities > 50 worms. The hypothesis of a crowding factor, acting alone, is not supported.

The hypothesis based on resource limitation (H_{a1}) agreed with observations at low and high intensities, while the hypothesis based on an intraspecific crowding factor (H_{a2}) agreed with observations at low and intermediate intensities. We simulated the combined effects of resource limitation and an intraspecific crowding factor by combining H_{a1} and H_{a2} into a third alternate hypothesis, H_{a3}. Confidence limits generated under H_{a3} (Fig. 7B) included all but 8 observations. The data are consistent with effects of intraspecific crowding at low intensities that are subordinate to effects of resource limitation at high intensities.

Summary of simulations on real data sets

In these examples, we evaluated natural or experimental data with a model assuming no density dependence. In some cases, this technique provided a clear indication of the absence or presence of density dependence, corresponding to conclusions reached by the original authors using other analytical procedures. In other cases, it identified intensities where more data are necessary, or where parameters may have been estimated incorrectly. We have also shown two examples of strong density dependence, one where the data suggest a single density-dependent phenomenon and another where we suspect a more complex interaction of multiple phenomena.

DISCUSSION

Tests for density dependence commonly involve regression analysis of *per capita* parasite productivity against intensity. Usually, few data points are available for the more heavily infected hosts due to aggregation of parasites in the host population (see for example Keymer & Slater, 1987), yet these few points will influence the regression strongly. Authors note also a high degree of variability in *per capita* productivity among lightly infected hosts (Dobson, 1986; Keymer & Slater, 1987; Shostak & Dick, 1987). This variability, together with limited data on the heavily infected hosts, can confound the interpretation of regression analyses. In this paper, we have presented a simple graphical technique that may aid the interpretation of such data sets.

Theoretical simulations produced similar patterns over a wide range of values for variables. Application to diverse real data sets produced C.L. that tracked, qualitatively, the shape and location of scatterplots of observed data. Quantitative agreement, allowing for errors in estimating variables using small samples from skewed distributions, was also good in most cases. We emphasize that these results do not verify the truth of the assumptions underlying the model. Rather, they show that predictions mimicking reality can arise from simple assumptions regarding the biological attributes of host and parasite individuals, and the manner by which those individuals come together to form host–parasite assemblages.

An intriguing result of the simulations concerns the shifting role of parasite and host variability as determinants of average *per capita* parasite productivity. In single-worm infections, with excess resources, variation among hosts in *per capita* parasite productivity reflects only the variation among parasites (including any density-independent host effect). Increased intensity reduces variability among hosts, since estimated *per capita* productivities are based on increasing sample size. The estimates converge toward the parasite population mean, as long as resources are in excess. When intensities increase such that resource limitations occur in some hosts, counter forces are acting. Some hosts still provide sufficient resources for all their parasites, but superimposed on this are other hosts that provide insufficient resources. Their capacity to provide resources is relatively low, and/or by chance they are infected by parasites with particularly high requirements. As intensity increases further, resource limitations soon occur in all hosts. Variation among individual parasites becomes irrelevant, and variation among hosts solely determines the magnitude of the variability in *per capita* parasite productivity, and the ability to detect density dependence. These results have practical significance. Data from low-intensity infections should provide an estimate of P_{max} that is free of density-dependent host effects. Data from high-intensity infections where density dependence is evident should provide an estimate of H_{max} that is free of the effects of variability among individual parasites.

The theoretical simulations showed that different subsets of assumptions produce predictable effects on the C.L., so an unusual pattern in the data can suggest which assumptions of the model might have been violated. One example comes from the case of

H. diminuta. Outlying observations suggested that density dependence acted differently than through the mechanism of resource limitation which was assumed in the basic model. The flexibility of our approach permitted the incorporation and testing of multiple mechanisms, requiring only a modification of the assumption of constant $\mu(P_{max})$. A second example comes from the case of *P. pinguis*. The C.L. generated by the model narrowed too rapidly with increasing intensity. Simulations showed that making the assumption that $\sigma(P_{max})$ is an increasing function of intensity can reduce the rate of narrowing of C.L. Infection dynamics may provide a biological basis for this assumption. Assume that lightly infected hosts are so because they have only recently acquired their parasites; their parasites would tend to be uniformly young (= small), and low $\sigma(P_{max})$ would be appropriate. More heavily infected hosts, presumably infected over a longer time span, would harbour parasites of increasingly mixed age (and size), and a higher $\sigma(P_{max})$ would be appropriate.

Our simulation protocol provides a means of predicting *per capita* parasite productivity at any intensity, given only P_{max}, H_{max}, and a function relating them. It predicts graphically the intensity where density dependence may be first showing its effects, in the absence of data from that intensity. This is particularly important for designing follow-up studies to clarify the situation. Hosts whose data will be most helpful to test hypotheses can be identified, and treatments may be allocated to subjects more optimally within experimental designs. It also predicts the complete distribution of hosts at different intensities. Although we chose to present only the C.L. for P_{avg}, the distributions generated by simulation permit the calculation of means, medians, variance, skewness, and other properties. This enhances the ability to discriminate among competing hypotheses, compared with techniques where only a single property (such as the mean) is used.

We fully recognize the simplicity of our approach. Features such as ontogeny, mate finding, immunity, and phenotypic plasticity in the expression of parasite life-history traits, have been condensed into the two 'black boxes' of H_{max} and P_{max}. Given the extraordinary complexity of the host–parasite interaction, together with intra-specific parasite interactions, it could be considered presumptuous that such a simple framework would have any applicability. However, since natural infections provide data only on the coarse scale of H_{max} and P_{max}, we believe that our approach holds promise for (i) evaluating survey data for evidence of density dependence, and (ii) generating specific hypotheses concerning mechanisms of density dependence, which can then be tested experimentally. Our simulation model can be used with survey data to generate expectations under a null hypothesis of no density dependence. In the absence of density dependence, there should exist a $\mu(P_{max})$ and $\sigma(P_{max})$ that generate C.L. which conform closely to observations on singly- and lightly-infected hosts. These variables, which then are estimated using only lightly infected hosts, enable the extrapolation of C.L. to higher intensities. Then, if even a single heavily infected host is present in a sample, its *per capita* parasite productivity can be evaluated relative to expectations under the null hypothesis. P_{max} may be estimated directly from data on singly-infected hosts. If many hosts are lightly infected, but few have single-parasite infections from which to estimate P_{max} directly, indirect estimation may be used. If $\boldsymbol{H_0}$ is true, then the $\mu(P_{max})$ should be the same at all intensities, and $\sigma(P_{max})$ can be estimated by back-calculation using observations from higher intensities, since it is related to $\sigma(P_{avg})$ and to intensity by equation (2*a*). Of course, one should guard against using data from intensities so high that density-dependent effects are evident.

An important caveat when using the simulation model to generate a quantitative null hypothesis is that the C.L. under the null hypothesis are only valid assuming that the values for the μ and σ of P_{max} are true. Confidence limits for estimates of means and standard deviations can be determined (Sokal & Rohlf, 1981), and a conservative approach might be to use a low estimate for $\mu(P_{max})$, and a high estimate for $\sigma(P_{max})$, as a null hypothesis. This will render density dependence more difficult to detect. We suspect, however, that poor estimates for P_{max} will most likely occur when sample sizes of hosts are too small to address the question of density dependency by any method. The same caveat applies when evaluating hypotheses of density dependence. The utility of C.L. that are generated depends upon the accuracy of the estimate of H_{max}, and the appropriateness of function chosen to relate P_{max} to H_{max}.

The evaluation of data from dioecious parasites requires additional assumptions regarding mating success, if fecundity is used to estimate P_{max}. In our example of *A. lumbricoides*, we assumed that a similar proportion of females at all intensities were mated (including the single-female infections from which we estimated P_{max}). A high proportion of unmated females in low-intensity infections could produce a low estimate of $\mu(P_{max})$ and a high estimate of $\sigma(P_{max})$. In combination, these would reduce the lower C.L. under the hypothesis of density independence, and render density-dependent effects more difficult to detect. If mating success was suspected to vary with intensity, constant μ and σ of P_{max} could be replaced by intensity-dependent functions.

Keymer & Slater (1987) identified various types of measurement errors that may make detection of density dependence more difficult. For example, if only one out of every two worms present is purged

following anthelmintic treatment, the estimated *per capita* fecundity is doubled, but the estimated intensity is halved, in each host. Our simulation procedure provides a framework that can be modified easily to explore the consequences of various types of procedural considerations.

Keymer & Slater (1987), and the present study, used different assumptions to simulate the effect of variability in *per capita* parasite fecundity on the ability to detect density dependence. Their simulation assumed that skewed *per capita* fecundities at low intensities reflects a skewed distribution of **host suitability**, and that the same *per capita* fecundity would occur in each host regardless of intensity. Consequently, high *per capita* fecundity is as likely to occur in heavily as in lightly infected hosts. By contrast, we assumed that the skewed distribution of observations at low intensities reflects a skewed distribution of **individual parasite productivity**. Our simulation predicts that high *per capita* fecundities become less likely as intensity increases. The real data sets examined by Keymer & Slater (1987), and in our study, support our prediction. We do not disregard the assumption of variation in host suitability (Keymer & Slater, 1987), but incorporate it into our model on the scale of the individual parasite. Our P_{max} describes parasite phenotypes that reflect a combined effect of parasite genetics and the environment provided by the host individual.

Our results clearly show, even in the absence of sampling bias and measurement errors, that natural variability among hosts and parasites makes density dependence more difficult to detect. However, they also show that this variability can be quantified using data from naturally infected hosts, and used to construct testable hypotheses on density dependence.

This research was supported by a Natural Sciences and Engineering Research Council of Canada (NSERC) grant (A3585) to M.E.S., and a NSERC Post-doctoral Fellowship and a Canadian Government Laboratories Visiting Fellowship to A.W.S. Research at the Institute of Parasitology is funded by NSERC and by the Fonds FCAR pour l'aide et le soutien à la recherche.

REFERENCES

COOK, R. L. & ROBERTS, L. S. (1991). *In vivo* effects of putative crowding factors on development of *Hymenolepis diminuta*. *Journal of Parasitology* **77**, 21–5.

DIETZ, K. (1988). Density dependence in parasite transmission dynamics. *Parasitology Today* **4**, 91–7.

DOBSON, A. P. (1985). Inequalities in the individual reproductive success of parasites. *Parasitology* **92**, 675–82.

HALL, A. (1982). Quantitative variability of nematode egg counts in faeces: a study among rural Kenyans. *Transactions of the Royal Society of Tropical Medicine and Hygiene* **75**, 682–7.

HESSELBERG, C. A. & ANDREASSEN, J. (1975). Some influences of population density on *Hymenolepis diminuta* in rats. *Parasitology* **71**, 517–23.

HOLLAND, C. V., CROMPTON, D. W. T., TAREN, D. L., NESHEIM, M. C., SANJUR, D., BARBEAU, I. & TUCKER, K. (1987). *Ascaris lumbricoides* infection in pre-school children from Chiriqui Province, Panama. *Parasitology* **95**, 615–22.

JACKSON, H. & TINSLEY, R. (1988). Environmental influences on egg production by the monogenean *Protopolystoma xenopodis*. *Parasitology* **97**, 115–27.

KEYMER, A. (1982). Density-dependent mechanisms in the regulation of intestinal helminth populations. *Parasitology* **84**, 573–87.

KEYMER, A. E. & SLATER, A. F. G. (1987). Helminth fecundity: density dependence or statistical illusion? *Parasitology Today* **3**, 56–8.

MEDLEY, G. & ANDERSON, R. M. (1985). Density-dependent fecundity in *Schistosoma mansoni* infections in man. *Transactions of the Royal Society of Tropical Medicine and Hygiene* **79**, 532–4.

PACALA, S. W. & DOBSON, A. P. (1988). The relation between the number of parasites/host and host age: population dynamics causes and maximum likelihood estimation. *Parasitology* **96**, 197–210.

READ, C. P. (1951). The 'crowding effect' in tapeworm infections. *Journal of Parasitology* **37**, 174–8.

ROBERTS, L. S. (1961). The influence of population density on patterns and physiology of growth in *Hymenolepis diminuta* (Cestoda: Cyclophyllidea) in the definitive host. *Experimental Parasitology* **11**, 332–71.

ROBERTS, L. S. & INSLER, G. D. (1982). Developmental physiology of cestodes. XVII. Some biological properties of putative 'crowding factors' in *Hymenolepis diminuta*. *Journal of Parasitology* **68**, 263–9.

SCOTT, M. E. & LEWIS, J. W. (1987). Population dynamics of helminth parasites in wild and laboratory rodents. *Mammal Review* **17**, 95–103.

SHOSTAK, A. W. (1986). Sources of variability in life-history characteristics of the annual phase of *Triaenophorus crassus* (Cestoda: Pseudophyllidea). Ph.D. thesis, University of Manitoba.

SHOSTAK, A. W. & DICK, T. A. (1987). Individual variability in reproductive success of *Triaenophorus crassus* Forel (Cestoda: Pseudophyllidea), with comments on use of the Lorenz curve and Gini coefficient. *Canadian Journal of Zoology* **65**, 2878–85.

SHOSTAK, A. W., ROSEN, R. B. & DICK, T. A. (1985). The use of growth curves to assess the crowding effect on procercoids of the tapeworm *Triaenophorus crassus* in the copepod host *Cyclops bicuspidatus thomasi*. *Canadian Journal of Zoology* **63**, 2343–51.

SINNIAH, D. (1982). Daily egg production of *Ascaris lumbricoides*; the distribution of eggs in the faeces and the variability of egg counts. *Parasitology* **84**, 167–75.

SMITH, G. (1984). Density-dependent mechanisms in the regulation of *Fasciola hepatica* populations in sheep. *Parasitology* **88**, 449–61.

SOKAL, R. R. & ROHLF, F. J. (1981). *Biometry*. 2nd Edn. San Francisco: W.H. Freeman and Company.

WAKELIN, D. (1986). Genetic and other constraints on resistance to infection with gastrointestinal nematodes. *Transactions of the Royal Society of Tropical Medicine and Hygiene* **80**, 742–7.

ZAVRAS, E. T. & ROBERTS, L. S. (1985). Developmental physiology of cestodes: cyclic nucleotides and the identity of putative crowding factors in *Hymenolepis diminuta*. *Journal of Parasitology* **71**, 96–105.